Polyhedron 157 (2019) 548–557

Contents lists available at ScienceDirect

Polyhedron

journal homepage: www.elsevier.com/locate/poly

# Synthesis of β-ketoiminate and β-iminoesterate tungsten (VI) oxo-alkoxide complexes as AACVD precursors for growth of $WO_x$ thin films

Xiaoming Su, Taehoon Kim, Khalil A. Abboud, Lisa McElwee-White *

*Department of Chemistry, University of Florida, Gainesville, FL 32611-7200, USA*

ARTICLE INFO

*Article history:*
Received 31 August 2018
Accepted 13 October 2018
Available online 24 October 2018

Dedicated to Prof. William D, Jones.

*Keywords:*
Tungsten oxide
Chemical vapor deposition
Single source precursors
metal oxo complexes
metal oxide films

ABSTRACT

The tungsten (VI) oxo-alkoxide complexes $WO(OR)_3L$ [R = $^t$Bu; L = acNac, etNac, tbNac, acNac$^{Me}$, acNac$^{Et}$] (**1**–**5**) and $WO(OCH_3)_3$(acNac) (**6**) have been synthesized. The isomeric purity of these complexes depends on the steric bulk of the substituent on the imino nitrogen of the chelating ligand. The thermal properties of the complexes have been evaluated to assess the effect of the β-ketoiminate or β-iminoesterate ligands. $WO(OC(CH_3)_3)_3$(acNac) (**1**) has been used as a precursor for aerosol assisted chemical vapor deposition (AACVD) of $WO_x$ thin films at temperatures from 250 to 450 °C. The results of mass spectrometry and thermolysis studies have been used to propose possible precursor decomposition pathways during film deposition.



## 1. Introduction

Tungsten oxide is an extensively investigated functional material for various applications such as electrochromic devices [1,2], sensing [3,4], catalysis [5–7] and organic electronics [8]. Besides the advantages of low cost, good chemical stability and mechanical flexibility, the wide application of tungsten oxide can also be attributed to its variety of phases (structural complexity) and stoichiometries (compositional complexity), which results in unique optical, electrical, photocatalytic and magnetic properties [9]. For example, $WO_{2.5}$ can be applied as an efficient electron and hole injection/transport layer in organic light-emitting diodes (OLEDs) [10], while $WO_{2.72}$ is an efficient catalyst for hydrogenation [5] and $WO_{2.9}$ shows great potential in HCHO sensing and elimination [11,12].

Due to the close relationship between physiochemical structures and materials properties, the ability to control stoichiometry, degree of crystallinity and morphology of $WO_x$ to meet the requirements for specific application is critical. Among the numerous $WO_x$ processing techniques including sol–gel, sputtering and thermal evaporation, chemical vapor deposition finds practical use due to its capability to deliver large-scale conformal coatings. Aerosol-assisted chemical vapor deposition (AACVD) is a variant of conventional CVD in which the precursor is dissolved in a solvent and then delivered to the reactor as an aerosol [13]. Therefore, AACVD relies on the solubility of the precursors instead of volatility, which offers greater flexibility in precursor design [14].

Ideal precursors for CVD would have adequate volatility (or solubility for AACVD), stability during the transport process to the reactor, clean decomposition and easy preparation [15]. Utilizing chelating ligands as a strategy to increase the volatility and stability of tungsten oxide precursors has been reported [16–19]. However, these studies are limited to the use of β-diketonate/β-ketoesterate and aminoalkoxide ligands. The β-ketoiminate/iminoesterate ligands are a very attractive class of mixed N,O-bidentate ligands for preparation of various metal complexes, which have been applied in medicinal chemistry [20], polymerization [21] and MOCVD [22–25]. Apart from easy preparation and good coordination ability, their steric and electronic properties can be tuned by altering the substituents on the backbone or the nitrogen. Due to the limited application of these ligands in designing $WO_x$ precursors, we have synthesized complexes of the type $WO(OR)_3L$ (R = $^t$Bu, Me) bearing various β-ketoiminate/β-iminoesterate ligands, which include 4-amino-3-penten-2-onate (acNac), 4-(methylamino)-3-penten-2-onate (acNac$^{Me}$), 4-(ethylamino)-3-penten-2-onate (acNac$^{Et}$), ethyl 3-aminocrotonate (etNac) and *tert*-butyl 3-aminocrotonate (tbNac) (see Scheme 1). We then studied AACVD of $WO_x$ thin films from $WO(OC(CH_3)_3)_3$(acNac) (**1**). To the best of our knowledge, this the first reported study in

* Corresponding author.
*E-mail address:* lmwhite@chem.ufl.edu (L. McElwee-White).

https://doi.org/10.1016/j.poly.2018.10.035
0277-5387/

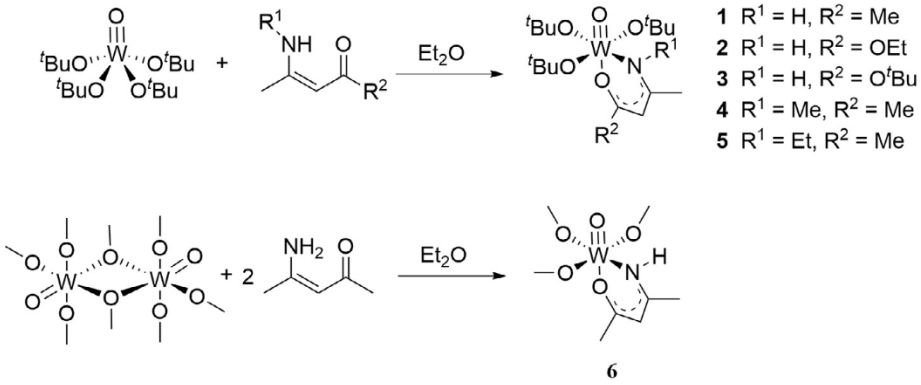


**Scheme 1.** Synthesis of complexes **1**–**6**.

which the N,O-bonding analogs of acac chelating ligands have been used in precursors for chemical vapor deposition of tungsten oxides.

## 2. Experimental

### 2.1. General considerations

All reactions were carried out under an inert atmosphere ($N_2$) employing conventional glovebox or standard Schlenk techniques. Methylene chloride, hexane and toluene (Fisher Scientific) were purified using an MBraun MB-SP solvent purification system and stored over activated 3 Å molecular sieves prior to use. Diethyl ether and tetrahydrofuran were dried using sodium/benzophenone, distilled, and stored over activated 3 Å molecular sieves prior to use. Hexamethyldisiloxane, methanol, chloroform-$d_1$ (Cambridge Isotopes) and benzene-$d_6$ (Cambridge Isotopes) were stored over 4 Å molecular sieves. Diethylamine was distilled over potassium hydroxide and stored over 4 Å molecular sieves. The compounds $WOCl_4$ [26], $WO[OC(CH_3)_3]_4$ [26], $[WO(OCH_3)_4]_2$ [27], acNacH [28], acNac$^{Me}$H [29], acNac$^{Et}$H [30], 4-*tert*-butylamino-3-penten-2-one (acNac$^{tBu}$H) [31], etNacH [28] and tbNacH [28] were synthesized according to literature procedures with modifications. All other solvents and reagents were of analytical grade and were used as received. NMR spectra were recorded on either a Varian Mercury 300BB (300 MHz) spectrometer or a Varian INOVA 500 spectrometer using residual protons from deuterated solvents for reference. Thermogravimetric analysis was performed using a TA Q5000 under an atmosphere of nitrogen at a temperature scan rate of 10 °C/min to 600 °C. Mass spectrometry was performed on a ThermoScientific DSQ II with direct insertion probe (DIP) using chemical ionization (CI) with methane as the reagent gas or electron ionization (EI) (70 eV) or a Bruker Daltonics Impact II-Qq-TOF instrument with electrospray as the source of ionization in positive mode. Elemental analyses were performed by Robertson Microlit Laboratories (Ledgewood, NJ).

### 2.2. Synthesis

#### 2.2.1. $WO(OC(CH_3)_3)_3$(acNac) (**1**)

In the glove box, $WO(OC(CH_3)_3)_4$ (2.093 mmol, 1.030 g) was dissolved in diethyl ether (30 mL) in a Schlenk flask and then transferred to the Schlenk line. 4-Amino-3-penten-2-one (2.108 mmol, 0.2090 g) was dissolved in diethyl ether (10 mL). The $WO(OC(CH_3)_3)_4$ solution was cooled to 0 °C in ice bath for 30 min, and the solution of 4-amino-3-penten-2-one was then added dropwise. The reaction mixture was then slowly warmed to room temperature after stirring for 30 min. The reaction was allowed to stir for 12 h, then the volatiles were removed under vacuum. The crude product was sublimed between 62 and 74 °C (50–100 mTorr) to obtain yellow solid. Yield: 0.715 g (66.0%). Crystals for X-ray crystallography were grown by cooling a toluene/hexane solution of complex **1** to −3 °C. $^1$H NMR ($C_6D_6$, 25 °C): $\delta$ 7.13 (b, 1H, NH), 4.75 (d, 1H, CHCO, $J$ = 1.7 Hz), 1.75 (s, 3H, $COCH_3$), 1.59 (s, 9H, C$(CH_3)_3$), 1.44 (s, 18H, C$(CH_3)_3$), 1.32 (d, 3H, $CH_3$C(NH), $J$ = 1.0 Hz). $^{13}$C NMR ($C_6D_6$, 25 °C): $\delta$ 181.26 ($COCH_3$), 168.95 (C(NH)), 99.76 ($CHCO(CH_3)$), 82.48 ($C(CH_3)_3$), 80.62 ($C(CH_3)_3$), 30.22 (($CH_3)_3$C), 30.74 (($CH_3)_3$C), 26.12 ($CH_3CO$), 25.60 ($CH_3$C(NH)). *Anal.* Calc. for $WO_5C_{17}H_{35}N$: C, 39.47; H, 6.82; N, 2.71. Found: C, 38.23, H, 6.34; N, 2.75%. MS (ESI) $m/z$ Calcd for $WO_5C_{17}H_{35}NK$ $[M+K]^+$: 556.1657. Found: 556.1634.

#### 2.2.2. $WO(OC(CH_3)_3)_3$(etNac) (**2**)

Compound **2** was synthesized following the same procedure as used for **1**. Starting with $WO(OC(CH_3)_3)_4$ (1.219 mmol, 0.6003 g) and etNacH (1.229 mmol, 0.1588 g), a yellow solid (0.5601 g, 84.0%) was obtained after removal of the volatiles under vacuum. The crude product was sublimed at 52–62 °C (100–140 mTorr) to afford a yellow product. Yield: 0.1425 g (23.5%). $^1$H NMR ($C_6D_6$, 25 °C): $\delta$ 6.41 (b, 1H, NH), 4.66 (d, 1H, CHCO, $J$ = 1.6 Hz), 4.04 (q, 2H, $CH_2CH_3$, $J$ = 7.1 Hz), 1.56 (s, 9H, C$(CH_3)_3$), 1.45 (s, 18H, C$(CH_3)_3$), 1.33 (s, 3H, $CH_3$C(NH)), 1.06 (t, 3H, $CH_3CH_2$, $J$ = 7.1 Hz). $^{13}$C NMR ($C_6D_6$, 25 °C): $\delta$ 170.96 ($COCH_2$), 168.89 (C(NH)), 82.98 ($CHCOCH_2$), 82.02 ($C(CH_3)_3$), 81.01 ($C(CH_3)_3$), 60.39 ($CH_2CH_3$), 31.05 (($CH_3)_3$C), 30.72 (($CH_3)_3$C), 26.19 ($CH_3$C(NH)), 15.01 ($CH_3$-$CH_2$). MS (ESI) $m/z$ Calcd for $WO_6C_{18}H_{37}NK$ $[M+K]^+$: 586.1762. Found: 586.1781.

#### 2.2.3. $WO(OC(CH_3)_3)_3$(tbNac) (**3**)

Compound **3** was synthesized following the same procedure as used for **1**. Starting with $WO(OC(CH_3)_3)_4$ (1.015 mmol, 0.4998 g) and tbNacH (1.023 mmol, 0.1608 g), a yellow solid (0.4422 g, 75.7%) was obtained after removal of the volatiles under vacuum. The crude product was sublimed at 59–62 °C (220–380 mTorr) to afford a yellow product. Yield: 0.1124 g (19.2%). $^1$H NMR ($C_6D_6$, 25 °C): $\delta$ 6.27 (b, 1H, NH), 4.60 (d, 1H, CHCO, $J$ = 1.6 Hz), 1.57 (s, 9H, C$(CH_3)_3$), 1.50 (s, 9H, $COC(CH_3)_3$), 1.44 (s, 18H, C$(CH_3)_3$), 1.32 (d, 3H, $CH_3$C(NH), $J$ = 0.6 Hz). $^{13}$C{$^1$H} NMR ($C_6D_6$, 25 °C): $\delta$ 171.78 ($COC(CH_3)_3$), 168.74 (C(NH)), 84.45 ($CHCOC(CH_3)_3$), 81.55 ($C(CH_3)_3$), 80.90 ($C(CH_3)_3$), 79.83 ($OC(CH_3)_3$), 31.06 (($CH_3)_3$C), 30.74 (($CH_3)_3$C), 29.16 (($CH_3)_3$C), 25.78 ($CH_3$C(NH)). MS (ESI) $m/z$ Calcd for $WO_6C_{20}H_{41}NK$ $[M+K]^+$: 615.210. Found: 615.2129.

#### 2.2.4. $WO(OC(CH_3)_3)_3$(acNac$^{Me}$) (**4**)

Compound **4** was synthesized following the same procedure as used for **1**. Starting with $WO(OC(CH_3)_3)_4$ (2.099 mmol, 1.0333 g) and acNac$^{Me}$H (2.105 mmol, 0.2382 g), a yellow solid (0.8806 g, 79.0%) was obtained after removal of the volatiles under vacuum.

The crude product (**4A** with traces of **4B**) was sublimed at 82–94 °C (100–200 mTorr) to afford a yellow solid, which is a mixture of **4A** and **4B** in ~1:3 ratio. Yield of the mixture: 0.5383 g (48.3%). Isomer **4A**: $^1$H NMR ($C_6D_6$, 25 °C): $\delta$ 4.85 (s, 1H, CHCO), 3.10 (s, $NCH_3$), 1.86 (s, 3H, $COCH_3$), 1.58 (s, 9H, $C(CH_3)_3$), 1.48 (s, 18H, $C(CH_3)_3$), 1.45 (s, 3H, $CH_3C(NCH_3)$). $^{13}$C NMR ($C_6D_6$, 25 °C): $\delta$ 170.34 ($COCH_3$), 167.26 ($C(NCH_3)$), 104.21 ($CHCO(CH_3)$), 82.56 ($C(CH_3)_3$), 80.96 ($C(CH_3)_3$), 39.50 ($N(CH_3)$), 30.97 (($CH_3)_3C$), 30.27 (($CH_3)_3C$), 25.07 ($CH_3CO$), 21.41 ($CH_3C(NCH_3)$). Isomer **4B**: $^1$H NMR ($C_6D_6$, 25 °C): $\delta$ 4.89 (s, 1H, CHCO), 3.41 (s, $NCH_3$), 1.77 (s, 3H, $COCH_3$), 1.58 (s, 9H, $C(CH_3)_3$), 1.43 (s, 18H, $C(CH_3)_3$), 1.40 (s, 3H, $CH_3C(NCH_3)$). $^{13}$C NMR ($C_6D_6$, 25 °C): $\delta$ 177.57 ($COCH_3$), 168.62 ($C(NCH_3)$), 104.03 ($CHCO(CH_3)$), 82.72 ($C(CH_3)_3$), 80.41 ($C(CH_3)_3$), 43.33 ($N(CH_3)$), 31.16 (($CH_3)_3C$), 30.75 (($CH_3)_3C$), 25.22 ($CH_3CO$), 21.92 ($CH_3C(NCH_3)$). *Anal.* Calc. for $WO_5C_{18}H_{37}N$ (mixture of **4A** and **4B**): C: 40.69; H: 7.02; N: 2.64. Found: C, 40.30; H, 6.77; N, 2.63%.

### 2.2.5. $WO(OC(CH_3)_3)_3(acNac^{Et})$ (**5**)

Compound **5** was synthesized following the same procedure as used for **1**. Starting with $WO(OC(CH_3)_3)_4$ (1.623 mmol, 0.7988 g) and $acNac^{Et}H$ (1.640 mmol, 0.2086 g), a yellow oil (0.5192 g, 58.7%) was obtained after removal of the volatiles under vacuum. The crude product was distilled at 82–90 °C (100–200 mTorr) to afford a yellow oil. Yield: 0.2895 g (32.7%). The isomer ratio of **5A** and **5B** is ~1:1 and they were not separated from one another. For the mixture of **5A** and **5B**: $^1$H NMR ($C_6D_6$, 25 °C): $\delta$ 4.85 (s, 1H, CHCO), 4.77 (s, 1H, CHCO), 3.85 (q, $NCH_2CH_3$, $J$ = 7.1 Hz), $\delta$ 3.57 (q, $NCH_2CH_3$, $J$ = 7.1 Hz), 1.82 (s, 3H, $COCH_3$), 1.75 (s, 3H, $COCH_3$), 1.58 (s, 9H, $C(CH_3)_3$), 1.55 (s, 9H, $C(CH_3)_3$), 1.54 (s, 3H, $CH_3C(NC_2H_5)$), 1.53 (s, 3H, $CH_3C(NC_2H_5)$), 1.45 (s, 18H, $C(CH_3)_3$), 1.41 (s, 18H, $C(CH_3)_3$), 1.33 (t, $NCH_2CH_3$, $J$ = 7.1 Hz), 1.16 (t, $NCH_2CH_3$, $J$ = 7.1 Hz). $^{13}$C NMR ($C_6D_6$, 25 °C): $\delta$ 177.10 ($COCH_3$), 169.24 ($COCH_3$), 168.09 ($C(NC_2H_5)$), 165.60 ($C(NC_2H_5)$), 104.01 ($CHCO(CH_3)$), 103.51 ($CHCO(CH_3)$), 82.67 ($C(CH_3)_3$), 82.40 ($C(CH_3)_3$), 81.02 ($C(CH_3)_3$), 80.70 ($C(CH_3)_3$), 50.18 ($N(CH_2CH_3)$), 46.09 ($N(CH_2CH_3)$), 31.08 (($CH_3)_3C$), 30.97 (($CH_3)_3C$), 30.85 (($CH_3)_3C$), 30.26 (($CH_3)_3C$), 25.32 ($CH_3CO$), 25.08 ($CH_3CO$), 21.62 ($CH_3C(NC_2H_5)$), 21.19 ($CH_3C(NC_2H_5)$), 16.39 ($N(CH_2CH_3)$), 15.42 ($N(CH_2CH_3)$). *Anal.* Calc. for $WO_5C_{19}H_{39}N$: C: 41.85; H: 7.21; N: 2.57. Found: C, 41.52; H, 7.21; N, 2.66%.

### 2.2.6. $WO(OCH_3)_3(acNac)$ (**6**)

Compound **6** was synthesized following the same procedure as used for **1**. Starting with $[WO(OCH_3)_4]_2$ (0.771 mmol, 0.4998 g) and acNacH (1.572 mmol, 0.1558 g), a yellow solid (0.4952 g, 82.0%) was obtained after removal of the volatiles under vacuum. The crude product was distilled at 70–74 °C (100–140 mTorr) to afford a yellow oil. Yield: 0.1695 g (28.1%). $^1$H NMR ($C_6D_6$, 25 °C): $\delta$ 7.36 (b, 1H, NH), 4.68 (s, 3H, $OCH_3$), 4.63 (d, 1H, CHCO, $J$ = 1.9 Hz), 4.41 (s, 6H, $OCH_3$), 1.75 (s, 3H, $COCH_3$), 1.18 (d, 3H, $CH_3C(NH)$, $J$ = 0.8 Hz). $^{13}C\{^1H\}$ NMR ($C_6D_6$, 25 °C): $\delta$ 182.40 ($COCH_3$), 171.30 (C(NH)), 100.87 ($CHCO(CH_3)$), 63.41 ($OCH_3$), 61.77 ($OCH_3$), 26.07 ($CH_3$), 25.55 ($CH_3$). *Anal.* Calc. for $WO_5C_8H_{17}N$: C: 24.57; H: 4.38; N: 3.58. Found: C, 24.36; H, 4.21; N, 3.61%.

## 2.3. $WO_x$ materials growth and characterization

$WO_x$ films were deposited onto silicon substrates with native silicon dioxide ($Si/SiO_2$, n-type, <100>) using a custom-built, vertical cold-wall impinging-jet AACVD reactor [32]. Substrates were cleaned in boiling acetone, ethanol and deionized water for 3 min each, and then placed on a SiC covered graphite susceptor in the reaction chamber under vacuum. Solutions of precursor **1** (0.034 M in diglyme) were prepared and loaded into a 10 mL gas-tight Hamilton syringe (4 mL h$^{-1}$ injection rate). Aerosol was generated from the precursor solution using a nebulizer with a quartz plate vibrating at 1.44 MHz and delivered to the reaction chamber with nitrogen (99.999% purity, Airgas) carrier gas at a flow rate of 1000 sccm. Deposition was conducted for 150 min, during which the reactor pressure was maintained at 350 Torr and the deposition temperature was controlled by a radio frequency (RF) heating system on the susceptor.

The elemental composition of $WO_x$ films was determined using ULVAC-PHI XPS Al Kα radiation after 2 min 2 kV $Ar^+$ sputtering to remove surface contaminants and oxygen was used as an internal standard set at 530.5 eV [16,33]. The Shirley base line was subtracted before peak fitting. The XPS spectra of the W 4f core level were fitted into peak doublets with parameters of spin–orbit separation $\Delta EP$ ($4f_{5/2}$–$4f_{7/2}$) = 2.18 eV. The intensity ratio of the W $4f_{7/2}$ and W $4f_{5/2}$ peak doublet was set to 4:3. The morphology of the films was examined using field emission scanning electron microscopy (FESEM, FEI Nova NanoSEM 430). The crystallinity was measured by X-ray diffraction (XRD, Panalytical X'pert Pro).

## 2.4. Crystallographic structure determination of **1**

X-ray Intensity data were collected at 100 K on a Bruker **DUO** diffractometer using Mo Kα radiation ($\lambda$ = 0.71073 Å) and an APEXII CCD area detector. Raw data frames were read by the program SAINT[1] and integrated using 3D profiling algorithms. The resulting data were reduced to produce *hkl* reflections and their intensities and estimated standard deviations. The data were corrected for Lorentz and polarization effects and numerical absorption corrections were applied based on indexed and measured faces.

The structure was solved and refined in SHELXTL*2014*, using full-matrix least-squares refinement. The non-H atoms were refined with anisotropic thermal parameters and all of the H atoms were calculated in idealized positions and refined riding on their parent atoms. The asymmetric unit consists of two crystallographically independent but chemically equivalent complexes. The amino proton from both complexes were obtained from a Difference Fourier map and refined freely. The second complex (W1b) has two disordered regions. In one, the three methyl groups bound to C10b are refined in two parts. In the second, the full ligand on O3b is refined in two parts as well. In both cases the site occupation factors were dependently refined. In the final cycle of refinement, 9941 reflections (of which 9078 are observed with $I > 2\sigma(I)$) were used to refine 483 parameters and the resulting $R_1$, $wR_2$ and $S$ (goodness of fit) were 2.72%, 5.51% and 1.064%, respectively. The refinement was carried out by minimizing the $wR_2$ function using $F^2$ rather than $F$ values. $R_1$ is calculated to provide a reference to the conventional $R$ value but its function is not minimized.

## 2.5. Thermolysis studies

Each compound (complex **1**, **2** and pure ligand acNacH) was placed in a 10 mL headspace vial with a septum and heated in the GC oven at 250 °C for 40 min. The oven was then cooled to 32 °C. Once cool, the headspace vial was removed from the oven. A 100-μL sample of the headspace gases was taken with a gas-tight syringe and injected in split mode for GC/MS. Mass spectrometry was conducted on a ThermoScientific (San Jose, CA) DSQ II using electron ionization (70 eV) and an ion source at 250 °C. Gas chromatography was conducted on a ThermoScientific Trace GC Ultra.

## 2.6. Adhesion test

The Scotch tape test was used to evaluate the adhesion of the deposited $WO_x$ films on native silicon dioxide ($Si/SiO_2$, n-type, <100>) substrates. A strip of commercial Scotch tape (Magic™, 3M) was attached to the deposited film and then peeled off. The film adhered to the substrate and not to the tape. Images of the

tape and the films before and after the test are in supplementary information (Fig. S8).

## 3. Results and discussion

### 3.1. Precursor design

Compounds of the type $WO(OR)_3L$ (R = alkyl; L = β-diketonate, β-ketoesterate) have been studied as $WO_x$ CVD precursors [16,17] but the research on tungsten complexes containing the structurally related β-ketoiminate or β-iminoesterate ligands has been very limited. β-Ketoiminates or β-iminoesterates have been successfully used as ligands in CVD precursors for metal oxide films including MgO [34], ZnO [35] and $Co_3O_4$ [36]. In contrast to the commonly used β-diketonate ligands, these mixed N/O chelating ligands provide more flexibility for controlling the physical and thermal properties of the complexes by tuning the substituents at the imino functionality or the backbone. Oxo and alkoxide groups have advantageous features in synthesizing single source metal oxide precursors. As O-bound ligands, they can serve as the oxygen source for materials growth. Tungsten-oxygen multiple bonding in the oxo ligands reduces bond cleavage requirements during deposition. Bulky *tert*-butoxide and the smallest alkoxide methoxide have been chosen as ligands in this study, to allow exploration of the influence of steric bulk and mixed N/O chelating ligands.

### 3.2. Synthesis

β-Ketoimines and β-iminoesters were synthesized by condensation reactions between the corresponding β-diketone/β-ketoester and a suitable amine source according to modified literature procedures [28,30]. The mononuclear complexes $WO(OR)_3L$ (R = alkyl, L = β-ketoiminate or β-iminoesterate) were prepared by addition of the bidentate ligand to $[WO(OMe)_4]_2$ or $WO(O^tBu)_4$ in ether (Scheme 1). After reacting at room temperature for 12 h, all volatiles were removed to give the crude product, which can be further purified by sublimation or distillation. Attempts to synthesize and purify $WO(OMe)_3L$ complexes where L = $acNac^{Me}$ or $acNac^{Et}$ failed, due to rapid decomposition of the products. The reactivity of β-ketoiminate ligands towards tungsten oxo alkoxide complexes is significantly affected by the steric bulk of their imino side chains. The N-$^t$butyl compound $acNac^{tBu}H$ does not react with $WO(O^tBu)_4$ or $[WO(OMe)_4]_2$ even at elevated temperature with increased reaction time.

### 3.3. X-Ray crystallographic structure determination of **1**

Single crystals of complex **1** that were suitable for molecular structure determination (Table 1) were grown by cooling a concentrated solution of **1** in toluene layered with hexane to −3 °C. There are two crystallographically independent but chemically equivalent molecules per asymmetric unit. One of the molecules is presented in Fig. 1. Selected bond angles and lengths are given in Table 2. Complex **1** exhibits a distorted octahedral geometry around the metal center with an equatorial plane defined by a *tert*-butoxide, the terminal oxo and the bidentate β-ketoiminate ligand. The other two chemically equivalent *tert*-butoxide ligands occupy non-linear axial positions (O5B-W1B-O3B, 163.96(16)°) bending away from the terminal oxo group. Besides the effect of steric repulsion, the distortion of normal octahedral geometry is also influenced by the strong multiple bonding of W–O(oxo), which is facilitated by the restricted bite angle of the chelating β-ketoiminate ligand (O2B-W1B-N1B, 79.41(13)°) [17,37].

Despite the possibility of isomers due to the unsymmetrical nature of the acNac ligand, complex **1** shows an exclusive *trans* geometry between the oxo ligand and O (O,O-*trans*) due to the *trans* effect of W–O(oxo) [37–39]. Compared with compounds of the type $[WO(OR)_3(acac)]$, whose W–O bonds trans to the oxo groups are typically ~2.2 Å [17], the analogous W1B–O2B bond

**Table 1**
Crystal data and structure refinements for **1**.

| | |
|---|---|
| Empirical formula | $C_{17}H_{35}NO_5W$ |
| Formula weight | 517.31 |
| Temperature | 100(2) K |
| Wavelength | 0.71073 Å |
| Crystal system | triclinic |
| Space group | $P\bar{1}$ |
| *Unit cell dimensions* | |
| $a$ (Å) | 10.4335(6) |
| $b$ (Å) | 13.5435(7) |
| $c$ (Å) | 15.4896(8) |
| $\alpha$ (°) | 95.753(1) |
| $\beta$ (°) | 95.922(1) |
| $\gamma$ (°) | 92.651(1) |
| $V$ (Å$^3$) | 2162.6(2) |
| $Z$ | 4 |
| $D_{calc}$ (Mg/m$^3$) | 1.589 |
| Absorption coefficient (mm$^{-1}$) | 5.364 |
| $F$(0 0 0) | 1032 |
| Crystal size (mm) | 0.221 × 0.095 × 0.044 |
| Theta range for data collection (°) | 1.906–27.499 |
| Index ranges | $-13 \le h \le 13$, $-17 \le k \le 17$, $-20 \le l \le 20$ |
| Reflections collected | 61 410 |
| Independent reflections ($R_{int}$) | 9941 (0.0166) |
| Completeness to theta = 25.242° | 100.0% |
| Absorption correction | numerical |
| Refinement method | Full-matrix least-squares on $F^2$ |
| Data/restraints/parameters | 9941/504/483 |
| Goodness-of-fit (GOF) on $F^2$ | 1.064 |
| Final $R$ indices [$I > 2\sigma(I)$] | $R_1$ = 0.0272, $wR_2$ = 0.0551 [9078] |
| $R$ indices (all data) | $R_1$ = 0.0310, $wR_2$ = 0.0579 |
| Extinction coefficient | n/a |
| Largest difference peak and hole (e Å$^{-3}$) | 5.508 and −3.202 |
| $R_1 = \sum(\|\|F_o\| - \|F_c\|\|)/\sum\|F_o\|$ | $wR_2 = [\sum[w(F_o^2 - F_c^2)^2]/\sum(w(F_o^2)^2]]^{1/2}$ |
| $S = [\sum[w(F_o^2)^2 - F_c^2)^2]/(n\text{-}p)]^{1/2}$ | $w = 1/[\sigma^2(F_o^2) + (m^*p)^2 + n^*p]$ |
| $p = [\max(F_o^2,0) + 2^*F_c^2]/3$, $m$ & $n$ are constants | |

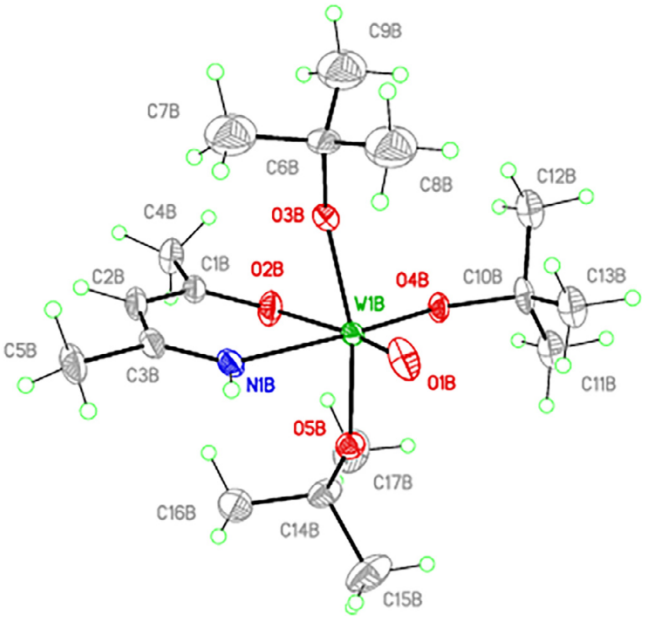


**Fig. 1.** A representation of **1** with thermal displacement ellipsoids shown at 40%.